

Effect of strain on the phase separation and devitrification of the magnetic glass state in thin films of $\text{La}_{5/8-y}\text{Pr}_y\text{Ca}_{3/8}\text{MnO}_3$ ($y = 0.45$)

This article has been downloaded from IOPscience. Please scroll down to see the full text article.

2010 J. Phys.: Condens. Matter 22 176002

(<http://iopscience.iop.org/0953-8984/22/17/176002>)

View the [table of contents for this issue](#), or go to the [journal homepage](#) for more

Download details:

IP Address: 129.252.86.83

The article was downloaded on 30/05/2010 at 07:55

Please note that [terms and conditions apply](#).

Effect of strain on the phase separation and devitrification of the magnetic glass state in thin films of $\text{La}_{5/8-y}\text{Pr}_y\text{Ca}_{3/8}\text{MnO}_3$ ($y = 0.45$)

V G Sathe, Anju Ahlawat, R Rawat and P Chaddah

UGC-DAE Consortium for Scientific Research, University Campus, Khandwa Road, Indore-452001, India

Received 20 November 2009, in final form 2 March 2010

Published 7 April 2010

Online at stacks.iop.org/JPhysCM/22/176002

Abstract

We present our study of the effect of substrate induced strain on $\text{La}_{5/8-y}\text{Pr}_y\text{Ca}_{3/8}\text{MnO}_3$ ($y = 0.45$) thin films grown on LaAlO_3 , NdGaO_3 and SrTiO_3 substrates that show large scale phase separation. It is observed that unstrained films grown on NdGaO_3 behave quite similarly to bulk material but the strained films grown on SrTiO_3 show melting of the insulating phase to the metallic phase at low temperatures. However, the large scale phase separation and metastable glass-like state is observed in all the films despite differences in substrate induced strain. The measurements of resistivity as a function of temperature under a cooling and heating in unequal field (CHUF) protocol elucidate the presence of a glass-like metastable phase generated due to kinetic arrest of the first order transformation in all the films. Like structural glasses, these magnetic glass-like phases show evidence of devitrification of the arrested charge order antiferromagnetic insulator (CO-AFI) phase to the equilibrium ferromagnetic metallic (FMM) phase with isothermal increase of magnetic field and/or iso-field warming. These measurements also clearly show the equilibrium ground state of this system to be FMM and the metastable glass-like phase to be AFI phase.

(Some figures in this article are in colour only in the electronic version)

1. Introduction

The leading current efforts to understand colossal magnetoresistance (CMR) effects in manganites center around inhomogeneities and first order insulator–metal transitions [1]. The first order transition gets significantly broadened with increasing quenched disorder present in the system. $\text{La}_{5/8-y}\text{Pr}_y\text{Ca}_{3/8}\text{MnO}_3$ (LPCMO) is one such highly studied system, where substitutional disorder leads to phase separation at the micrometer length scale. Many researchers believe it to be a result of quenched disorder due to variation in ionic size of the constituent elements [2]. On the other hand, magnetic force microscopy studies elucidated fluid-like growth of the ferromagnetic metal (FMM) phase [3]. The presence of coexisting phases is an essential phenomena across any first order transition and disorder makes the transition broad, making coexistence of different phases possible for a sufficiently broad temperature and spatial range. In LPCMO

the two coexisting phases are charge order antiferromagnetic insulator (CO-AFI) and FMM. These series of materials show re-entrant transitions in magnetization and resistivity measurements that are not well understood [4–7]. Uehara *et al* [4] studied the relaxation behavior and observed that the value of resistivity strongly depends on the cooling rate. They described the phase separated states as strain glass states [5]. Sharma *et al* also described the low temperature state, in which CO-AFI and FMM phases coexist as strain glass-like magnetism [5] while Ghivelder *et al* classified the phase separation as dynamic phase separation and frozen phase separation [8, 9]. Dhakal *et al* [6] studied the magnetic field versus temperature ($H-T$) phase diagram and further observed these two distinct types of phase separation, a strain-liquid (dynamic phase separation) and a strain glass (frozen phase separation) region. It is argued that in the phase separated scenario the two phases are of nearly the same energy and the balance can be changed by external stimuli like magnetic field,

laser photons etc. It is shown that the CO-AFI state of this system can be converted to the FMM state by application of external stimuli such as magnetic field, current, voltage, laser photons, etc at low temperature. However, the system does not transform back to its original AFI state when the external field is withdrawn isothermally [7]. This naturally raises the question of whether the CO-AFI is the equilibrium state or the remnant state FMM is the equilibrium state? Thus a unified understanding is lacking that can explain the different phase separated phases and role of strain on the phase fraction ratio below the phase transition temperature apart from describing the correct ground state of the system.

It has previously been suggested that the strain parameter can tune the metal–insulator phase fraction in this LPCMO series of compounds [10]. Further, recently it is argued that the observed micro(meso) meter scale phase separation owes its existence to extrinsic causes like strain [11]. It is also remarked that ‘kinetic arrest’ could be another possible reason for the observed micrometer scale phase separation in manganites. Glass-like arrest of kinetics across first order magnetic transition has been reported in materials ranging across intermetallics and colossal magnetoresistance manganites [12–19] and they are known as magnetic glasses. The first order phase transition can be fully or partially arrested at low temperatures; the arrest occurs as one cools below a temperature T_g called the magnetic glass transition temperature, which is concurrent with the classical liquid glass transition temperature when one cools the liquid at a higher rate so that one passes the transition temperature without crystallization. This frozen state gets ‘de-arrested’ over a range of temperature as it is warmed, showing devitrification [13, 16, 17]. Depending on the system, the glass-like arrested state can be antiferromagnetic [13–16] or ferromagnetic [12, 13, 17, 18]. Thus it is interesting to study the role of strain and ‘kinetic arrest’ in an LPCMO compound that shows micrometer scale phase separation. One way of introducing strain into the compounds is to grow highly oriented thin films on different substrates. In the present study LPCMO films are grown on three substrates of NdGaO_3 (NGO), SrTiO_3 (STO) and LaAlO_3 (LAO) that provide three different values of strain in the films.

In this paper, it is shown that in this system the CO-AFI phase obtained as a majority state on cooling in $H = 0$, shows all the characteristics of a glassy state, including devitrification on warming. The recently designed ‘cooling and heating in unequal fields’ (CHUF) protocol [20] has been used to show that devitrification occurs whenever the sample is warmed in a magnetic field (H_w) that is higher than the field (H_c) it was cooled in; a re-entrant CO-AFI to FMM to CO-AFI transition is seen on heating as devitrification at T_g is followed by the first order transition at T^{**} analogous to melting at T_m [20]. Here we show that while T^{**} rises with increasing H (as expected), T_g falls with rising H similar to what is observed in the $\text{Pr}_{0.5}\text{Ca}_{0.5}\text{Mn}_{0.975}\text{Al}_{0.025}\text{O}_3$ (PCMAO) system [21].

2. Experimental details

In this study, we have used oriented thin films of $\text{La}_{5/8-y}\text{Pr}_y\text{Ca}_{3/8}\text{MnO}_3$ ($y = 0.45$) grown on commercially

procured SrTiO_3 , NdGaO_3 , and LaAlO_3 single crystal substrates using a pulsed laser deposition system. We have chosen this well-studied $y = 0.45$ composition which shows a photoinduced transition [7]. The lattice parameter of the bulk material nearly matches with the NGO(110) substrate (3.835 Å) thus the strain imparted on the film is very low (<0.4%). On the other hand, the lattice parameter of the LAO(100) substrate (3.79 Å) is smaller than that of the bulk lattice, imparting an in-plane compressive strain of 1.4% and the lattice parameter of the STO(100) substrate (3.905 Å) is larger than the bulk, giving an in-plane tensile strain of 1.6%. The polycrystalline sample for making the target in the pulsed laser deposition process was prepared by the standard solid state reaction method and is well characterized by Rietveld analysis of the x-ray powder diffraction data and Raman spectroscopy. The lattice parameters obtained from the Rietveld analysis (orthorhombic unit cell) are found to be $a = 5.435$ Å, $b = 7.663$ Å and $c = 5.4285$ Å. The films were prepared using a 248 nm KrF laser source operating at 3 Hz frequency and ~ 2 J cm⁻² energy density on the target. The thickness of all the films was kept around 200 nm. The chamber was evacuated initially to 1×10^{-7} Torr pressure while depositions were carried out in the partial oxygen pressure of 300 mTorr and the substrate was kept at 700 °C. After deposition the films were annealed in the same oxygen pressure for 30 min before slow cooling to room temperature. The films were well characterized by the x-ray diffraction method. The resistivity (ρ) measurements were carried out by the standard four probe method where magnetic field and current directions were kept parallel to each other. The typical current value was 1 μA for all the samples.

3. Result and discussions

Figure 1 shows standard θ –2θ x-ray diffraction patterns of films deposited on STO, NGO and LAO, respectively. The diffraction data shows that the films are perfectly oriented and of a single chemical phase and very good crystalline quality. A small peak is observed around 42.5° that corresponds to a contribution to the main peak from the Cu Kβ line. From peak positions of the substrate and films the strain parameter is calculated. From the position of the x-ray diffraction peaks of the films and substrate it is observed that the films grown on LAO have in-plane compressive strain while films on STO possess in-plane tensile strain. The film grown on NGO has a very small amount of strain and the lattice parameter nearly matches that of the bulk compound.

In order to study the metal–insulator transition and the associated phase separation phenomena, detailed resistivity measurements as a function of temperature have been carried out. The CO-AFI state and FMM transformation is reflected in resistivity measurements with orders of magnitude changing when the CO-AFI (high resistance) state is transformed to the FMM (low resistance) state through first order phase transition. The ρ versus T data for the three LPCMO films grown on STO, NGO and LAO are shown in figure 2 for cooling in 0 T to 5 K and subsequent warming, and cooling in 2 T to 5 K (FCC) and subsequent warming (FCW).

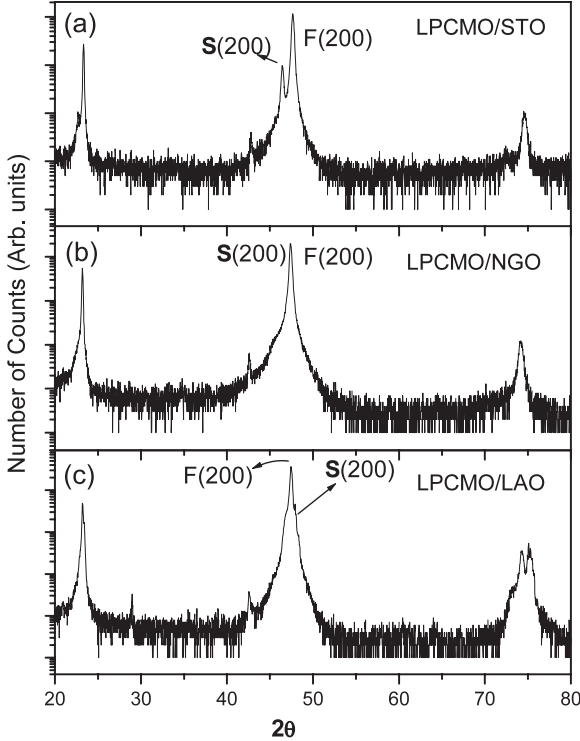


Figure 1. X-ray diffraction pattern of thin films of LPCMO grown on (a) STO, (b) NGO and (c) LAO substrates, respectively (top to bottom). The data are collected in normal powder diffraction geometry. S(200) and F(200) denotes the (200) peak of the substrate and film, respectively.

The effect of substrate induced strain is clearly seen in the resistivity data. For films on NGO and LAO (figures 2(b) and (c)) the zero field resistivity showed insulating behavior down to 100 K and remains higher than our measurement limit down to 5 K. The warming curve for these samples overlapped with the cooling curve. However, the cooling and warming curve of the resistivity for $H = 2$ T showed a clear insulator to metal transition and large hysteresis as highlighted for the film on NGO substrate in figure 2(d) where resistivity is plotted on a linear scale. This indicates first order transition from AFI to FMM phase under applied magnetic field. On the other hand, the films on STO showed a first order transition even for $H = 0$. The transition temperature T_C for $H = 0$ during cooling cannot be specified precisely as the resistance value is beyond our measurement limits but it lies near 50 K. The zero field measurements also showed large hysteresis between the cooling and warming curve confirming first order transition. The transition shifts to higher temperature when a 2 T field is applied and the transition temperature is close to that observed for NGO for the same field value. In short, the least strained film (<0.4% lattice mismatch) grown on NGO showed behavior similar to bulk material [22]. The behavior also matches that reported in [7] on exactly the same composition film grown also on NGO substrate. The in-plane compressed film grown on LAO (1.4% lattice mismatch) showed enhanced CO-AFI phase fraction while the in-plane tensile strained film grown on STO (1.6% lattice mismatch) showed suppression of the CO-AFI phase with a metal-insulator transition near 50 K.

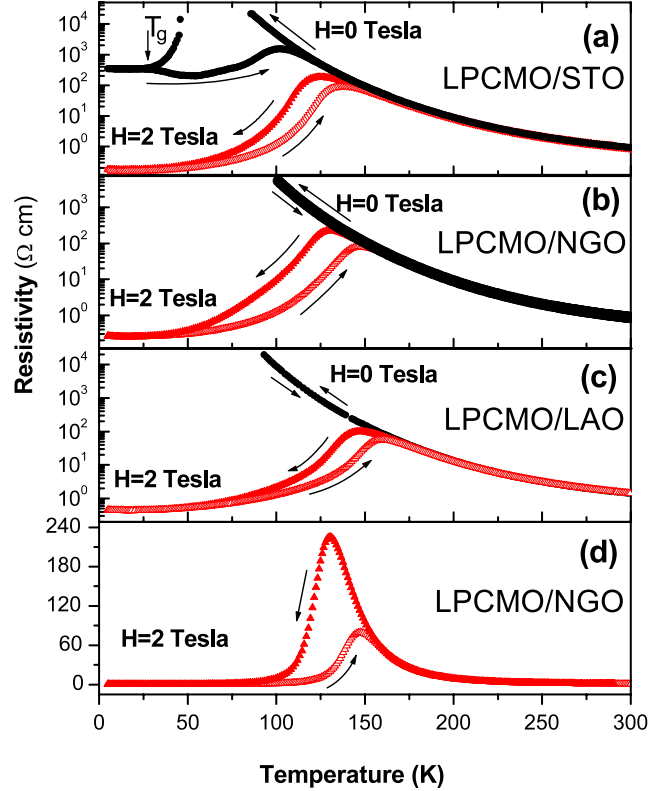


Figure 2. Resistivity versus temperature curves for thin films of $\text{La}_{5/8-y}\text{Pr}_y\text{Ca}_{3/8}\text{MnO}_3$ ($y = 0.45$) on (a) STO substrate, (b) NGO substrate and (c) LAO substrate for $H = 0$ and 2 T cooling and subsequent warming. (d) NGO substrate for 2 T cooling and subsequent warming on a linear scale. Cooling and warming directions are indicated by arrows.

Thus, it is shown that the strain does affect the observed phase coexistence in $H = 0$.

Uehara *et al* [22] have carried out a detailed study for various y ; for cooling in 0 T they observed a FMM phase at low T for $y < 0.275$; a partial conversion to FMM for $0.3 < y < 0.4$ and no conversion to FMM for $y > 0.41$. Bulk samples corresponding to our $y = 0.45$ film show no insulator to metal transition [7, 22]. It must be noted, however, that detailed measurements following novel paths in $H-T$ space established that $y = 0.41$ has an FMM ground state in $H = 0$ [14, 15, 23, 24]. With this background we use the recently designed CHUF protocol to investigate what the $H = 0$ ground state is for both our unstrained (NGO) and strained (STO, LAO) thin films.

As previously reported [8, 22, 25–28], this compound behaves as a phase separated system below T_C , with coexisting CO-AFI and the FMM phases. The zero field cooled state of the LPCMO/STO sample below ~ 30 K shows an entirely different behavior. The resistivity is nearly constant below this temperature both in the cooling and warming curve (see figure 2(a)). This suggests that the sample is frozen in a metastable state. This temperature is called the freezing temperature T_g . Such an anomalous behavior in the $H = 0$ resistivity curve below 30 K has been reported previously by many workers and attributed to different mechanisms.

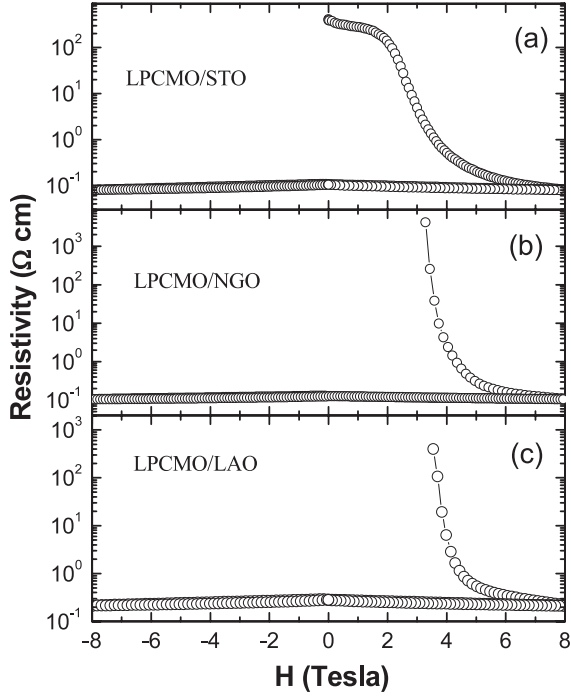


Figure 3. Magnetoresistance data of (a) LPCMO/STO film, (b) LPCMO/NGO film and (c) LPCMO/LAO film collected at 5 K.

Ghivelder *et al* [8] defined this state as a highly blocked state, with a small and almost time-independent fraction of FM phase in a matrix of CO-AFI phase. Sharma *et al* [5] labeled this state as a strained glass state, showing the highly glassy nature of the charge/spin degrees of freedom, and suggested that the re-entrant transition could be caused by a small free-energy difference between the competing FM and CO states. Recently, it has been shown in these families of compounds [23, 24] that the static phase coexistence persists to lower temperature without any change in phase fraction and is attributed to glass-like arrest of transformation kinetics that is frozen at T_g . It is worth mentioning here that this ‘magnetic glass’ state is completely different from spin glass, re-entrant spin glass or cluster glass. In magnetic glass, long range structural and magnetic order is always maintained but the kinetics of a first order transition is arrested and the high temperature magnetic phase is retained below T_g . This is similar to the conventional glass where the high temperature disordered phase is arrested below the glass transition temperature avoiding first order liquid to crystalline phase transition. In real systems, particularly like LPCMO where the doping induced disorder is large, the first order transition is very broad, spurring the partial transformation of the high- T phase upon cooling while the remaining fraction falls out of equilibrium and persists down to the lowest temperature as a glass-like arrested state.

In order to further investigate the nature of phase coexistence and glass-like behavior below ~ 30 K observed in figure 2, detailed magnetoresistance (MR) measurements were carried out by following various paths in $H-T$ space. Figure 3 shows the isothermal magnetoresistance measurement at 5 K for all the three samples. For these measurements samples were cooled under zero field to 5 K and magnetic

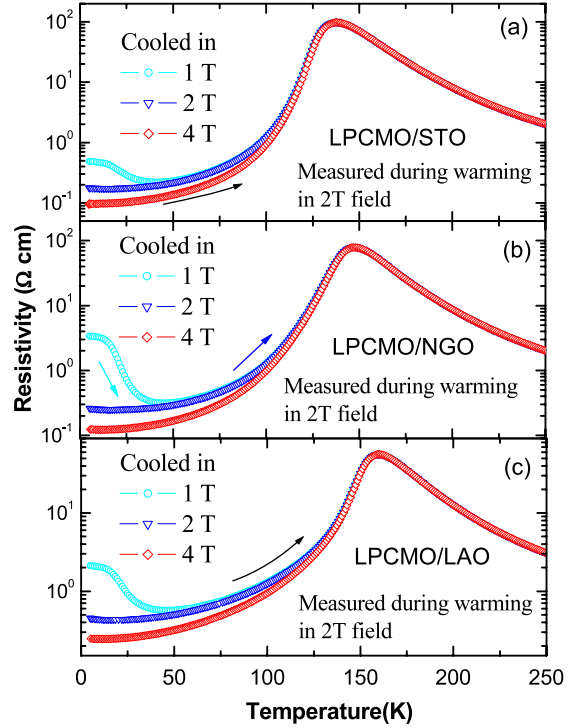


Figure 4. Resistivity as a function of temperature during warming in the presence of 2 T magnetic field for (a) LPCMO/STO, (b) LPCMO/NGO and (c) LPCMO/LAO. For each of these measurements samples are cooled in different magnetic fields of 1 T, 2 T and 4 T, respectively.

field is applied isothermally from $0 \rightarrow +8$ T (virgin curve) and then $+8 \rightarrow -8$ T $\rightarrow +8$ T (envelope curve). As can be seen from this figure, where resistivity is plotted on a log scale, the resistivity of films on NGO and LAO becomes measurable for magnetic fields higher than ~ 3 T and decreases by four order of magnitude by further increasing the magnetic field up to 8 T. This indicates a magnetic field induced transition from the CO-AFI to FMM state. Similar behavior is observed for an STO sample where resistivity is measurable at zero field and shows sharp changes in resistivity above 1.5 T magnetic field, indicating a field induced metal insulator transition. Besides four orders of magnitude change in the virgin curve, resistivity during the field reducing cycle from 8 to 0 T remains almost constant, suggesting the absence of a reverse transformation to the CO-AFI state. In fact there is almost negligible variation in resistivity for the entire envelope curve. This behavior, open hysteresis loop and virgin curve lying outside the envelope curve in resistivity, is similar to that observed in $\text{Pr}_{0.5}\text{Ca}_{0.5}\text{Mn}_{0.975}\text{Al}_{0.025}\text{O}_3$ (PCMAO) and some of the intermetallics [16, 20, 21]. There it is attributed to hindered kinetics of the first order transition at low temperature. In our case we obtain an almost AFI state when 5 K is reached in zero field conditions whereas we obtain an almost FM state at 5 K after field cycling.

To address which of these states (CO-AFI or FMM) are equilibrium states, we used the CHUF protocol as has been used earlier to address such issues [20] and is shown in figures 4 and 5. Under this protocol in one case (figure 4) the

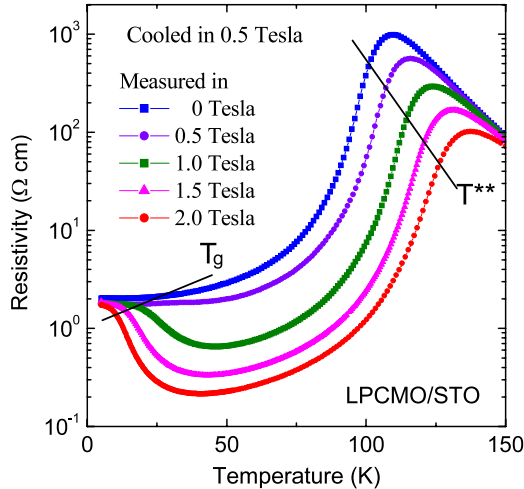


Figure 5. Resistivity as a function of temperature during warming in the presence of different magnetic fields for LPCMO film deposited on STO. For each of these measurements the sample is cooled in the presence of 0.5 T magnetic field to 5 K and the magnetic field changed to the labeled field value isothermally. Devitrification at low temperature and reverse transformation to the AFM state is highlighted. The dashed line shows T_g and the T^{**} line for these curves. See the text for details.

sample is cooled in different fields that are lower or higher than the warming field and then warmed in one field (2 T) while in the second case (figure 5) the sample is cooled in one field and then warmed in different field values lower and higher than the cooling field value. As shown in figure 4, the $\rho(T)$ curve during warming in the presence of 2 T and cooled in a field of 1 T showed a flat region for all the three samples at lowest temperature followed by a sharp decrease, indicating a CO-AFI to FMM transformation. The $\rho(T)$ then starts increasing again, finally showing an FMM to CO-AFI transition around 150 K. Whereas, for cooling fields of 2 and 4 T resistivity curves show only one transition around 150 K. As mentioned before when cooled in zero field to 5 K the system behaves as phase separated states, a combination of AFI and FMM phases and cooling in different fields changes the phase fraction of the two phases, as reflected in the different values of the resistivity at 5 K. The main feature that emerges from this figure is below ~ 30 K. When the samples are warmed in fields that are lower than the cooling fields, the resistivity shows an anomalous flat region followed by a sharp decrease before increasing with increasing temperature. This is analogous to the devitrification process observed in a classical glass transition. This behavior indicates the presence of a blocked CO-AFI state. This blocked glassy state melts on increasing temperature and crystallizes in the stable FMM state, resulting in a sharp fall in resistivity. On the other hand, ρ versus T curves under magnetic fields that are equal or higher than the cooling fields show behavior typical of an FMM phase. We can thus conclude that the FMM state is the equilibrium stable state of this system while the CO-AFI state is the metastable glassy state that coexists with it when measurements are performed under small fields. It also shows that one can tune the glass-like CO-AFI phase fraction at 5 K by varying the cooling field which is analogous to pressure in

a liquid to glass transition. A closer look at the devitrification curves (figure 4 (cooled in 1 T, warmed in 2 T)) for all the three films shows that the devitrification process is completed at lower temperature in film on STO, as compared to films on LAO and NGO. This lower value of T_g results in the part transformation of the CO-AFI phase to the FMM phase that is observed in zero field measurements for films on STO (see figure 2(a)).

In a liquid to glass transition, besides the cooling or quenching rate, pressure has been used as an additional parameter to form glasses, as in the vitrification of Ge with pressure [29]. Similar to these studies we used magnetic field to tune glass-like AFI states. The AFI phase obtained as a dominant state on cooling in $H = 0$, shows all the characteristics of a glassy state including devitrification on warming. When the samples are cooled in constant field and warmed in different fields, the devitrification of the blocked glassy state is highlighted and is shown in figure 5. Cooling the sample from 300 to 5 K in a field of 0.5 T results in coexisting phases; a stable equilibrium phase and metastable glass state. Now warming the sample in different fields provides an opportunity to study the process of the devitrification behavior of the magnetic glass and the dependence of T_g on H . It is observed that when warmed in fields lower than or equal to the cooling field the devitrification process is not observed and the heating curve shows monotonous increase in resistivity with increasing temperature. On the other hand when the sample is warmed in fields higher than the cooling field, devitrification of the glass-like CO-AFI phase to crystalline FMM phase is seen through a sharp decrease in ρ that starts at 17 K and terminates at ~ 46 K, with the mid-point of ρ (T_g at 1 T) being at ~ 25.6 K. The re-entrant transition, corresponding to melting of the FMM phase, is seen by a sharp increase in ρ , with the mid-point of transition (T^{**} at 1 T) being at 114 K. The sample is again cooled from 300 to 5 K in a cooling field of $H_C = 0.5$ T to obtain the same initial state and CO-AFI phase fraction and then warmed from 5 K after increasing field to $H_W = 1.5$ T. The devitrification for the FMM phase is again seen through a sharp drop in ρ that now starts at 11 K and terminates at about 41 K, with the mid-point of ρ (T_g at 1.5 T) being about 18.5 K. The mid-point of the re-entrant transition, corresponding to melting (T^{**} at 1.5 T) is 121 K. The same procedure is repeated but now with a warming field of 2 T and this results in a drop in ρ starting at 6 K and terminating at 39 K, with the mid-point of ρ (T_g at 2 T) being about 13.5 K. The mid-point of the re-entrant transition, corresponding to melting (T^{**} at 2 T) is 127 K. We see that T^{**} rises with increasing field so that an isothermal increase of H would, in a specific range of T , convert the CO-AFI state to FMM. The value of dT^{**}/dH must be consistent with the Clausius–Clapeyron relation since this is a first order transition. It is also noted that T_g at 1 T is 25 K, while that at 2 T is 10 K. T_g thus falls with increasing field, and an isothermal increase of H would, in a certain range of T , convert the glass-like CO-AFI phase to equilibrium FMM phase by devitrification. This is consistent with the qualitative condition imposed by Le Chatelier's principle, in that increasing H takes the system to a state with higher M . Such a behavior of T_g has also been observed for PCMAO [21].

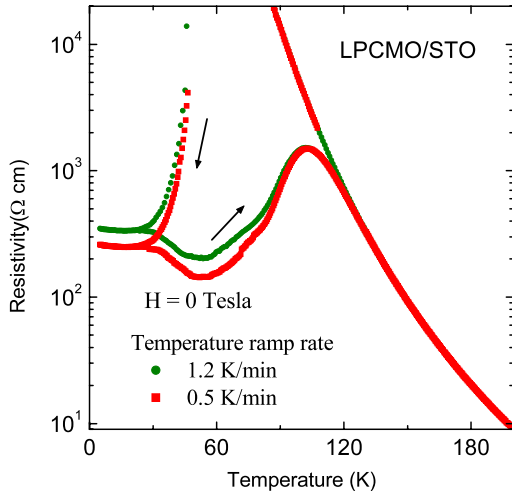


Figure 6. Resistivity as a function of temperature for $\text{La}_{5/8-y}\text{Pr}_y\text{Ca}_{3/8}\text{MnO}_3$ ($y = 0.45$) films deposited on STO with two different cooling rates. The resistivity at low T becomes smaller when the specimen is cooled slowly.

In a classical liquid to glass transition, avoiding first order transition, the cooling rate is very important. The faster the rate of cooling the more the fraction of the glass phase in the total system will be. In fact we can totally avoid the liquid to crystal-like first order transition with a sufficiently high cooling rate that varies from system to system. In order to elucidate the effect of the cooling rate on the present magnetic glass-like phase we carried out the cooling rate dependent ρ versus T measurements on the LPCMO/STO sample shown in figure 6. The upper curve shows the warming $\rho(T)$ curve after cooling from 300 to 5 K at a rate of 1.2 K min^{-1} . The next curve represents a $\rho(T)$ cooling curve measured at a rate of 0.5 K min^{-1} . It is observed that the value of ρ at 5 K decreases as the rate of cooling decreases, indicating a decrease in the glass-like CO-AFI phase as the rate of cooling is decreased. In short the relative volume fraction of CO-AFI with respect to the FMM phase decreases when the system is cooled more slowly across the first order transition and the associated timescale is in hours. This observation corroborates well with the normal glass transition.

4. Final remarks

It is worth noting here that in all the films of LPCMO, deposited on different substrates, such as NGO, STO and LAO, the glass-like arrest of kinetics is observed irrespective of strain. As mentioned before, the film deposited on NGO is the least strained as the lattice parameter of the NGO(110) substrate (3.859 \AA) nearly matches the lattice parameters of the LPCMO bulk compound. On the other hand, film deposited on STO shows an in-plane tensile strain while film on LAO shows in-plane compressive strain. The $\rho(T)$ data for all the films show glass-like behavior below $\sim 25 \text{ K}$. The substrate induced strain affects the magnitude of the resistivity in the films and thereby affects the first order CO-AFI to FMM transition temperature. The long range CO state is enhanced

with in-plane compressive strain and suppressed with in-plane tensile strain. Our observation contradicts earlier studies carried out on $y = 0.3$ samples, where tensile strain enhances the CO-AFI state [30]. We believe that this may be due to a difference in compositional variation; $y = 0.45$ and 0.3 compositions studied in the two cases. In the $y = 0.45$ composition the CO-AFI phase dominates and the system remains insulating down to the lowest temperature while for the $y = 0.3$ composition the FMM phase is in prominence at low temperatures, thus showing an insulator to metal transition at depleted temperatures [22]. However, the first order metal-insulator transition temperature values and hysteresis in heating and cooling under a magnetic field of 2 T are very close for the three films (see figure 2). This clearly shows that the ‘kinetic arrest’ across the first order transition retains its importance in shaping the large scale phase coexistence and at least in the LPCMO system seems to win over external effects like strain.

5. Conclusions

In summary, we performed an investigation of the low temperature transport properties of a micrometer length scale dynamic phase separated system, $\text{La}_{5/8-y}\text{Pr}_y\text{Ca}_{3/8}\text{MnO}_3$ ($y = 0.45$) thin films grown on NGO, STO and LAO substrates with the emphasis on understanding the roles of strain and ‘kinetic arrest’ across first order transitions. We have shown that phase separation is sensitive to the influence of the substrate induced strain. The long range CO-AFI state gets stronger with compressive in-plane strain and is suppressed with tensile strain. The resistivity versus temperature measurements under the CHUF protocol showed that the kinetics of first order phase transition is arrested across a CO-AFI to FMM transition and the arrested state behaves as a magnetic glass. Like structural glasses, these magnetic glass-like phases show evidence of devitrification of the arrested CO-AFI phase to the equilibrium FMM phase with isothermal increase of magnetic field and/or iso-field warming. Using the CHUF protocol it is shown that CO-AFI is the arrested metastable state while FMM is the equilibrium state of the system. The cooling rate dependent resistivity measurements further support the existence of a glass-like state in the system. Such a glass-like state and large scale dynamic phase separation is observed in all three film irrespective of their different substrate induced strains. Thus in LPCMO ‘kinetic arrest’ dominates over strain in shaping large scale phase separation.

Acknowledgments

We acknowledge Suresh Bhardwaj for help in x-ray diffraction measurements and Sachin Kumar for help in resistivity measurements.

References

- [1] Dagotto E 2005 *New J. Phys.* **7** 67
- [2] Dagotto E 2005 *Science* **309** 257
- [3] Zhang L, Israel C, Biswas A, Greene R L and de Lozanne A 2002 *Science* **298** 805

- [4] Uehara M and Cheong S-W 2000 *Europhys. Lett.* **52** 674
- [5] Sharma P A, Kim S B, Koo T Y, Guha S and Cheong S-W 2005 *Phys. Rev. B* **71** 224416
- [6] Dhakal T, Tosado J and Biswas A 2007 *Phys. Rev. B* **75** 092404
- [7] Chaudhuri S and Budhani R C 2008 *Europhys. Lett.* **81** 17002
- [8] Ghivelder L and Parisi F 2005 *Phys. Rev. B* **71** 184425
- [9] Sacanell J *et al* 2006 *Phys. Rev. B* **73** 014403
Macia F *et al* 2007 *Phys. Rev. B* **76** 174424
Macia F *et al* 2008 *Phys. Rev. B* **77** 012403
- [10] Ahn K H, Lookman T and Bishop A R 2004 *Nature* **428** 401
- [11] Shenoy V B, Gupta T, Krishnamurthy H R and Ramakrishnan T V 2009 *Phys. Rev. B* **80** 125121
(arXiv:[0904.1886v1](#))
Shenoy V B, Gupta T, Krishnamurthy H R and Ramakrishnan T V 2007 *Phys. Rev. Lett.* **98** 097201
- [12] Chattopadhyay M K, Roy S B and Chaddah P 2005 *Phys. Rev. B* **72** 180401R and references therein
- [13] Banerjee A, Mukherjee K, Kumar K and Chaddah P 2006 *Phys. Rev. B* **74** 224445
Banerjee A, Pramanik A K, Kumar K and Chaddah P 2006 *J. Phys.: Condens. Matter* **18** L605
- [14] Wu W, Israel C, Hur N, Soonyong P, Cheong S-W and De Lozane A 2006 *Nat. Mater.* **5** 881
- [15] Macia F, Abril G, Hernández-Mnguez A, Hernandez J M, Tejada J and Parisi F 2007 *Phys. Rev. B* **76** 174424
- [16] Roy S B, Chattopadhyay M K, Chaddah P, Moore J D, Perkins G K, Cohen L F, Gschneidner K A and Pecharsky V K 2006 *Phys. Rev. B* **74** 012403
Roy S B, Chattopadhyay M K, Banerjee A, Chaddah P, Moore J D, Perkins G K, Cohen L F, Gschneidner K A and Pecharsky V K 2007 *Phys. Rev. B* **75** 184410
- [17] Chaddah P, Kumar K and Banerjee A 2008 *Phys. Rev. B* **77** 100402R
- [18] Kushwaha P, Rawat R and Chaddah P 2008 *J. Phys.: Condens. Matter* **20** 022204
Kushwaha P, Lakhani A, Rawat R, Banerjee A and Chaddah P 2009 *Phys. Rev. B* **79** 132402
- [19] Banerjee A, Rawat R, Mukherjee K and Chaddah P 2009 *Phys. Rev. B* **79** 212403
- [20] Banerjee A, Kumar K and Chaddah P 2009 *J. Phys.: Condens. Matter* **21** 026002
Dash S, Banerjee A and Chaddah P 2008 *Solid State Commun.* **148** 336
- [21] Lakhani A, Kushwaha P, Rawat R, Kumar K, Banerjee A and Chaddah P 2010 *J. Phys.: Condens. Matter* **22** 032101
- [22] Uehara M, Mori S, Chen C H and Cheong S-W 1999 *Nature* **399** 560
- [23] Sharma P A, El-Khatib S, Mihut I, Betts J B, Migliori A, Kim S B, Guha S and Cheong S-W 2008 *Phys. Rev. B* **78** 134205
- [24] Kumar K, Pramanik A K, Banerjee A, Chaddah P, Roy S B, Park S, Zhang C L and Cheong S-W 2006 *Phys. Rev. B* **73** 184435
- [25] Yakubovskii A, Kumagai K, Furukawa Y, Babushkina N, Taldenkov A, Kaul A and Gorbenko O 2000 *Phys. Rev. B* **62** 5337
- [26] Garashenko A, Furukawa Y, Kumagai K, Verkhovskii S, Mikhalev K and Yakubovskii A 2003 *Phys. Rev. B* **67** 184410
- [27] Lee H J, Kim K H, Kim M W, Noh T W, Kim B G, Koo T Y, Cheong S-W, Wang Y J and Wei X 2002 *Phys. Rev. B* **65** 115118
- [28] Kim K H, Uhera M, Hess C, Sharma P A and Cheong S-W 2000 *Phys. Rev. Lett.* **84** 2961
- [29] Bhat M H, Molinero V, Soignard E, Solomon V C, Sastry S, Yarger J L and Angell C A 2007 *Nature* **448** 787
- [30] Gillaspie D, Ma J X, Zhai H-Y, Ward T Z, Christen H M, Plummer E W and Shen J 2006 *J. Appl. Phys.* **99** 08S901